PARAMETRIC FLUTTER ANALYSIS OF STRUT BRACED WING AIRCRAFT FOR REGIONAL AVIATION

Ana C. Meinicke[1], Roberto G. A. da Silva[1], and Patrice L. Guedes[2]

[1] Aeronautics Institute of Technology
Praça Marechal Eduardo Gomes, 50, São José dos Campos, SP Brazil
anameinicke@yahoo.com.br
gil@ita.br

[2] Embraer S. A.
Av. Brg. Faria Lima, 2170, São José dos Campos, SP Brazil
patrice.london@embraer.com.br

Keywords: strut-braced, flutter, parametric, regional aviation.

Abstract: The design of the conventional configuration of commercial aircraft, composed by a tube fuselage, a cantilever wing and an empennage, has been improved since its introduction in the 1950s and it is unlikely that great improvements should occur without drastic changes. The strut braced wing aircraft presents itself as an option. The main difference lies on a strut connecting the wing to the fuselage, reducing the bending moment of the wing and, consequently, its weight. Alternatively, the wing span could be increased, or even the wing thickness decreased, without great weight penalties. This combination of geometric changes reduces drag and improves performance. To evaluate possible aeroelastic issues that might hinder the development of this configuration, a parametric flutter analysis is performed based on aircraft of regional aviation size. As a result it was observed that: (a) increasing the wing aspect ratio from 8.3 to 12 decreases the flutter speed in 20%; (b) if the engine is positioned exactly at the wing and strut intersection at 70% of the wing span instead of 50%, an increase of 30% in flutter speed is obtained; (c) and that the flutter speed can be increased by 35% if the spanwise wing and strut intersection is moved from 70% to 30 % of the span.

1 INTRODUCTION

The design of the conventional configuration of commercial aircraft, composed by a tube fuselage, a cantilever wing, a vertical and a horizontal tail, has been improved since its introduction in the 1950s, and it is unlikely that great improvements should occur without drastic changes.

The strut braced wing (SBW) aircraft presents itself as an option. The main difference lies on a strut connecting the wing to the fuselage, reducing the bending moment of the wing and, consequently, its weight. Furthermore, the wing span could be increased, and the wing thickness decreased without great weight penalties. This combination of geometric changes reduces drag and improves performance.

Drag and weight parametric analyses were previously performed between the SBW and the conventional aircraft configurations, based on a regional aviation mission [1]. Drag reductions of 12% were obtained when comparing the SBW against a conventional aircraft of similar

size and weight, and 36% when comparing an SBW of aspect ratio 14 against a conventional aircraft of aspect ratio 8.3.

The aeroelastic performance of some truss braced wing (TBW) configurations was previously investigated by Bhatia et al [2]. The TBW consists of the SBW with an added jury (or more juries) between the wing and the strut. It was observed that increasing the span of the wing reduces its natural frequencies and, consequently, its flutter speed. However, designing a strut with different sweep angle than the wing tends to present a beneficial structural influence. In 2012 Bhatia et al. [3] performed a set of parametric studies on the TBW configuration to analyze the influence of the wing geometry parameters on the wing aeroelastic characteristics. The parameters considered were: wing span, strut sweep, spanwise location of wing and strut intersection, and number of truss members. It was observed that adding more juries improved flutter performance.

As observed by Coggin et al. [4], regarding the TBW aeroelastic effects, the truss and the juries present a significant influence on the structural modes and frequencies of the deformed structure. If a pre-stressed structure is considered, different results are obtained when compared to the traditional flutter analysis of the undeformed structure. By using a nonlinear aeroelastic solution, an increase in the flutter speed was observed, and for some cases, no flutter instability at all.

Sulaeman [5] investigated the effect of the compressive force provided by the strut on the inner part of the wing on the aeroelastic stability of the SBW. A sensitivity study was performed for the wing flutter speed according to several design variables. It was concluded that the compressive force presents a detrimental effect to the wing flutter speed and this effect is significant if the wing and strut intersection is placed near the wing tip.

As presented by Sulaeman [5], the SBW presents different aeroelastic characteristics when compared to those of a conventional aircraft. This is due to the addition of the strut and its influence on the aerodynamic loads, the mass and stiffness distributions, and to the usually higher aspect ratio and smaller wing thickness that optimized SBW aircraft present.

To verify if the SBW configuration presents unexpected and undesired aeroelastic characteristics, a parametric flutter analysis is performed. A parametric analysis provides better understanding of the configuration, especially early on in a non-conventional design since the accuracy of the models is still not high. It is interesting because it might shed a light on geometrically where the main problems of the configuration lie, and serves as a necessity to detail the aircraft from an aeromechanical point of view.

It must be noted that the main advantage of the SBW aircraft comes from the improvements in its aerodynamics. Its weight and aeroelastic characteristics are merely a consequence. The objective of the present analysis is to perform a preliminary investigation on its aeroelastic characteristics and it is not to be considered as a designing tool.

2 METHODOLOGY

The aeroelastic model developed for the flutter analysis consists of a finite element lumped mass model connected through splines to a Doublet Lattice Method (DLM) model, solved in MSC/Nastran, through a non-matched '*p*-*k*' solution.

The Finite Element Model (FEM) consists of beam elements, concentrated masses and rigid bars connecting the beams to the masses in such a way that they form the leading and trailing edges of the lifting surfaces. It is based on the Generic Narrow-Body Airliner (GNBA) developed by Guimarães Neto [6], except for the wing and strut parts. Hence, the fuselage and tail are conventional, but the wing and strut were modeled according to mass and stiffness values obtained from the structural mass model presented by Nagshineh-Pour [7].

The thickness value obtained through the double plate model [7] is used to obtain the wing cross section properties. However, the double plate model is not appropriate to calculate the wing cross section parameters for the flutter analysis since it does not provide any torsional stiffness. Thus, a hexagonal box is calculated from the wing thickness obtained, as presented by Sulaeman [5].

The wing was discretized in 35 grid points, which are the centroids of the cross sections. The material is considered isotropic, and its properties can be seen in Table 1.

Table 1: Aluminum alloy properties.

Density	2856 kg/m³
Young's Modulus	72 MPa
Allowable Stress	383.6 MPa

The strut is modeled as a beam element, with consistent mass, and a concentrated mass representing a telescoping mechanism, that allows the strut to only be active in positive *g* maneuvers, that is, traction [7]. The intersection between wing and strut is given at the modeled elastic axis.

The fixation between wing and fuselage is given in a *V* shape, as can be seen in Figure 1, since this provides a more realistic representation and behavior for a high wing configuration. This is necessary since the fuselage is modeled as beam elements, hence the intersection between wing and fuselage would be one point only if the *V* shape was not used.

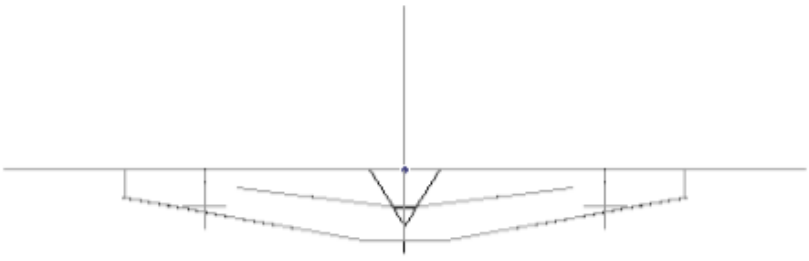

Figure 1: FEM model with reduced elements indicating the *V* shape connection between wing and fuselage

In the DLM model the lifting surfaces are assumed to lie parallel to the undisturbed flow, and divided into trapezoidal elements, called boxes, with its edges parallel to the free stream. The number of chordwise boxes on the lifting surfaces is defined such that the typical chord length $\Delta x < 0.08\ V/f$, where V is the minimum speed and f is the maximum frequency, as proposed in the Nastran user's guide. Indeed, as recommended in the Nastran Quick Reference Guide and by Rodden et al. [8], $\Delta x = 0.02\ V/f$ should be used to achieve convergence of force coefficients, this being a requirement for 50 chordwise boxes per wavelength. Also according to Rodden et al. [8], the box aspect ratio should be no greater than 10 to guarantee accuracy. For conservative purposes a maximum aspect ratio of 5 was used.

It is important to note that, since some parts of the strut lie very near to the wing, they present spanwise divisions that lie along those of the wing, and since the strut intersects the wing, the chordwise divisions in that region match as well.

To transfer the displacements from the structural nodes to the aerodynamic degrees of freedom, which commonly do not coincide, an interpolation method is used. In this analysis, surface and linear splines are employed. Infinite-plate splines were used for all lifting surfaces, fuselage, engines and pylons. Beam splines were used for the strut, since it was modeled as a beam and thus presents collinear grids.

In order to be able to use the surface splines, a fishbone structure was added to the FEM for the fuselage and the engines. This is done by adding grids and rigid bars connecting them to the main structure.

The flutter solution is obtained using the Nastran '*p-k*' method, where for each inputted speed the frequency and damping of each mode is calculated. These values are then analyzed through the *V-g-f* plots, where it is possible to see how the frequency and damping of each mode changes with the air speed. Flutter is observed at the lowest speed that damping is zero. Usually the frequency of two or more modes (including the one that presented zero damping) coalesce, meaning one mode is exciting the other through the air flow causing unstable oscillations.

The flutter speed analysis was performed for the SBW typical flight condition, which is, cruise at Mach 0.8 and 35000 ft.

A standard wing based on common regional aircraft is defined as a baseline, as can be seen in Table 2, where S represents area, the subscript w represents wing, AR is aspect ratio, Λ is the quarter-chord sweep angle, λ is the taper ratio, e_p is the engine spanwise position, t is the thickness, c is the chord, r_n is the nacelle radius and d is the fuselage diameter.

Table 2: Wing baseline parameters.

Parameter	Baseline Value
S_w	95 m²
AR_w	8.3
Λ_w	23°
λ_w	0.31
e_p	0.5
$(t/c)_{w\ avg}$	9%
r_n	1 m
d	3.5 m

A baseline strut was obtained based on the literature recommendations [9], and is defined in Table 3, where the subscript s represents strut, η is the dimensionless spanwise position of the wing and strut intersection, R is the relation between strut and wing area, L is the strut offset length and A_{cr} is the strut structural cross-sectional area.

The parameters varied in the analysis are the wing aspect ratio, engine spanwise position, strut offset length, strut sweep angle, spanwise wing and strut intersection, wing sweep and wing taper ratio. For simplification, only linear effects were accounted for in the structural and aerodynamic modeling, since this usually presents conservative results [4]. One last parameter

analyzed is the strut force, which can cause a pre-stress on the structure. For this case, the addition of the loads provided by the strut are going to be considered.

Table 3: Strut baseline parameters.

Parameter	Baseline Value
Λ_s	23°
λ_s	1
η	0.7
R	0.25
$(t/c)_{s\ avg}$	7%
L	1 m
A_{cr}	9.12 x 10^{-4} m²

3 RESULTS

When performing a flutter analysis it is always good practice to evaluate the natural frequencies and mode shapes of the structural dynamic model. Hence, a modal analysis is performed on the standard SBW. The four first elastic mode shapes and their respective natural frequencies can be seen in Figure 2.

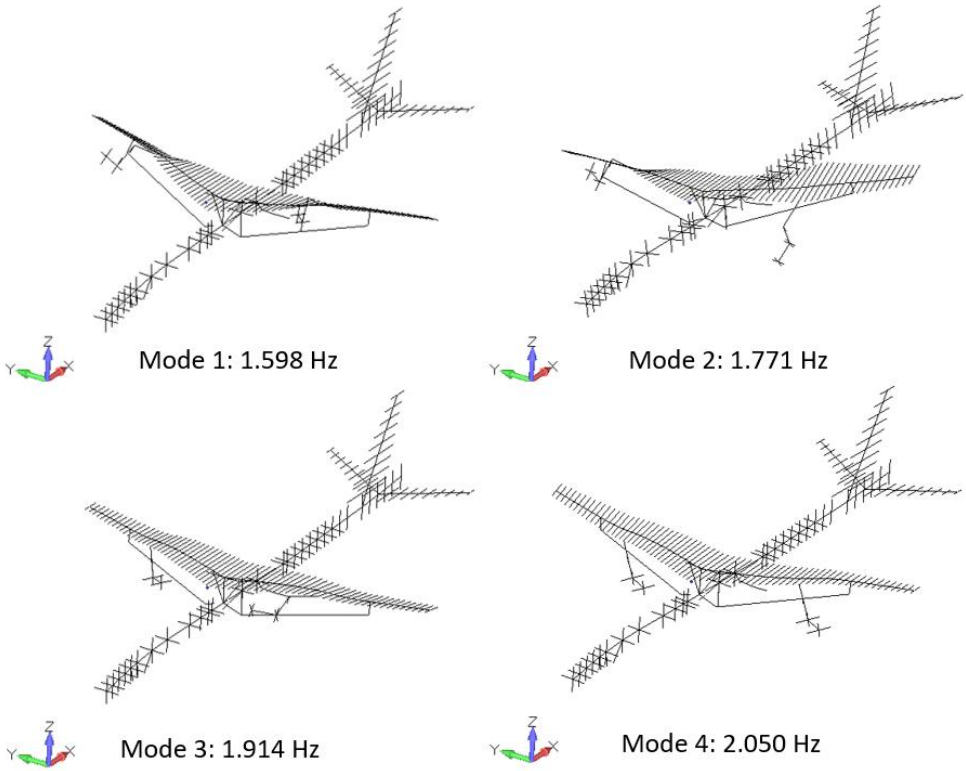

Figure 2: Baseline SBW first mode shapes and frequencies.

It is important to note that for each geometric variation the modes order, shapes and frequencies might change, and the analysis is still relevant.

The flutter speed observed is adimensionalized, as can be seen in Figure 3, and at that speed there seems to be a coalescence of modes 19 and 22, both symmetric. Mode 22 presented zero damping at a frequency of 7.18 Hz.

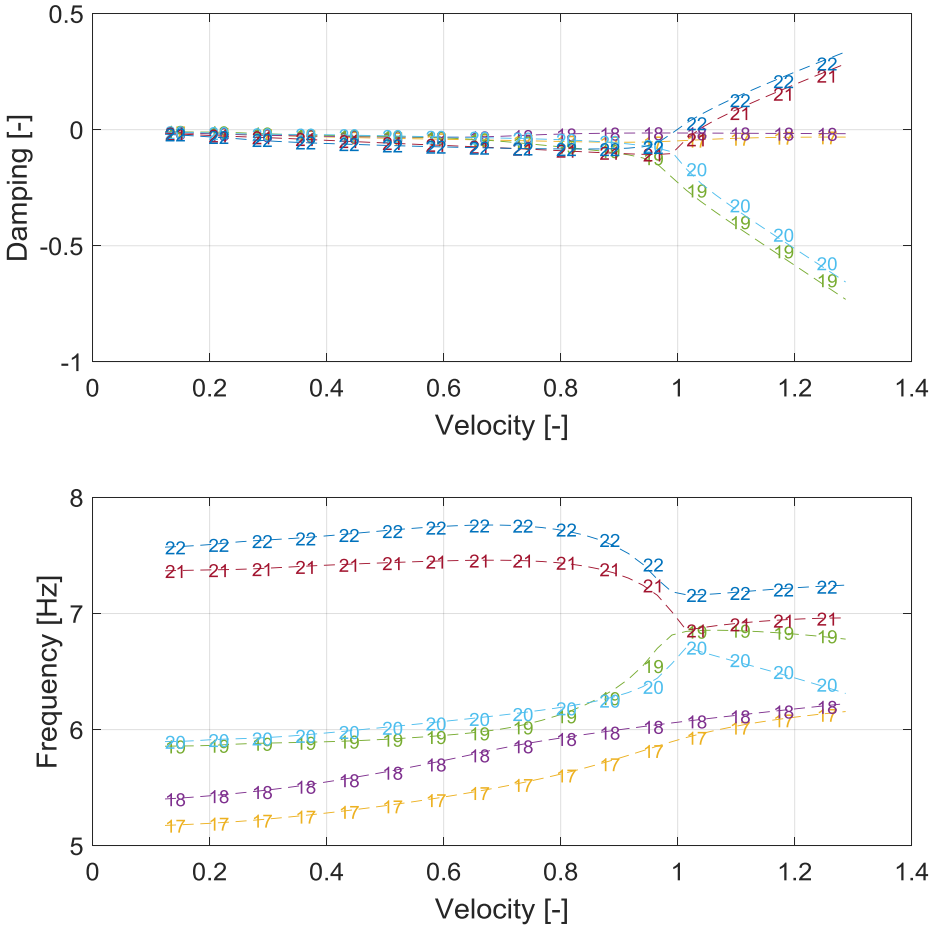

Figure 3: The V-g-f plot of the standard SBW for the modes close to the flutter frequency.

For the parametric analysis, the wing aspect ratio was varied from values of 6 up to 14. The aeroelastic models for each of the variations can be seen in Figure 4. The results can be seen in Figure 5, and it can be observed that the flutter speed decreases as the aspect ratio increases.

It is interesting to note that the flutter mechanism changes, for some points being caused by symmetric modes whereas in other by antisymmetric modes, and the flutter frequency decreases. This is expected, since higher aspect ratio leads to wings of higher span, these usually more flexible and/or heavier, and consequently lower frequencies and lower flutter speeds.

The next analysis consists of the variation of the engine position across the wing span, from 0.1 to 0.9. The aeroelastic model for each of the variations can be seen in Figure 6. The results can be seen in Figure 7, and it is observed that the closer the engine position is to the wing and strut intersection the higher the flutter speed. The intersection between wing and strut provides a higher local stiffness in that region, hence if the engine is positioned there, the aircraft presents a higher flutter speed.

The next analysis consists of performing variations on the length of the strut offset, from 0 to 1 m. The aerodynamic model for each of the variations can be seen in Figure 8.

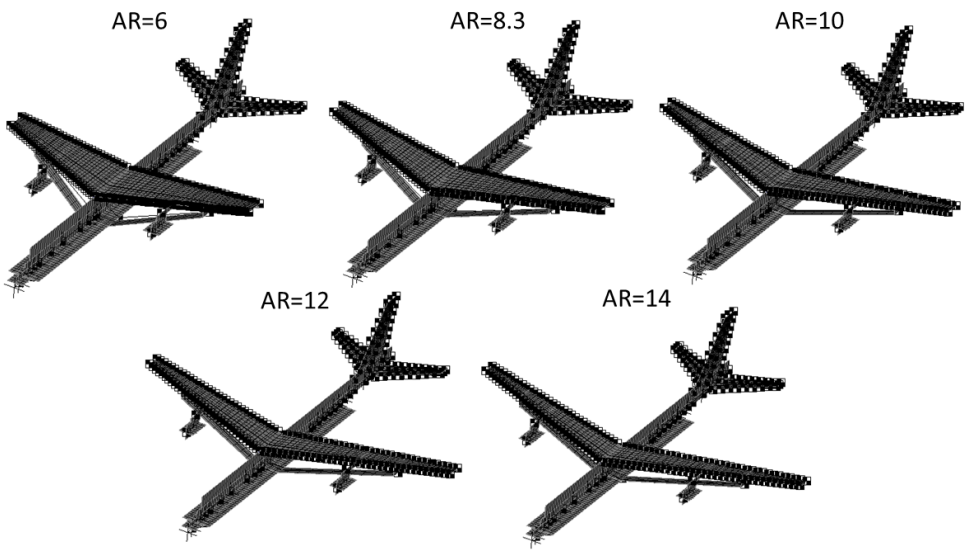

Figure 4: DLM and FEM model of the SBW with aspect ratio variation.

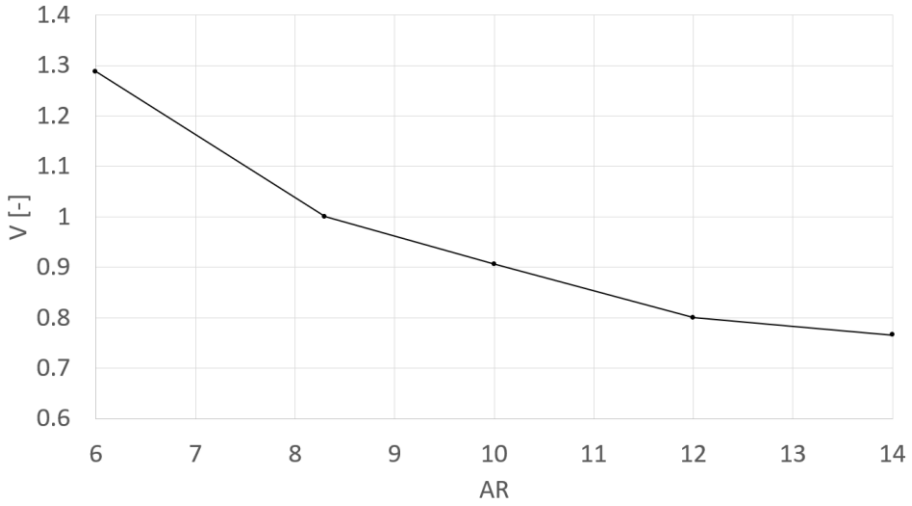

Figure 5: Nondimensional flutter speed as a function of wing aspect ratio.

The results can be seen in Figure 9. In general, the longer the strut offset the lower the flutter speed. This behavior was also observed by Sulaeman [5], even though there are conceptual differences between both analyzed aircraft. It seems that the offset can be beneficial to the structure, however, the longer the strut offset, the lower the stiffness of the structure. For this case there is only one major change in flutter mechanism from antisymmetric to symmetric modes for offset values up to 0.4 m and then for those over 0.6 m.

The strut sweep angle was varied from 16° to 32°, as can be seen in the geometric variations of Figure 10. The intersection of the wing and strut was kept the same, thus, as the sweep angle increases, the intersection between strut and fuselage approaches the aircraft nose.

The change in flutter speed according to the strut sweep angle can be seen in Figure 11. It can be observed that there is no clear trend, that is, the structure behavior changes for each strut sweep angle. However, when observing the modes that are present in the flutter mechanism, trends can be obtained when the mechanism is the same for two consecutive angle values. For these particular cases, the flutter speed seems to decrease as the sweep angle increases.

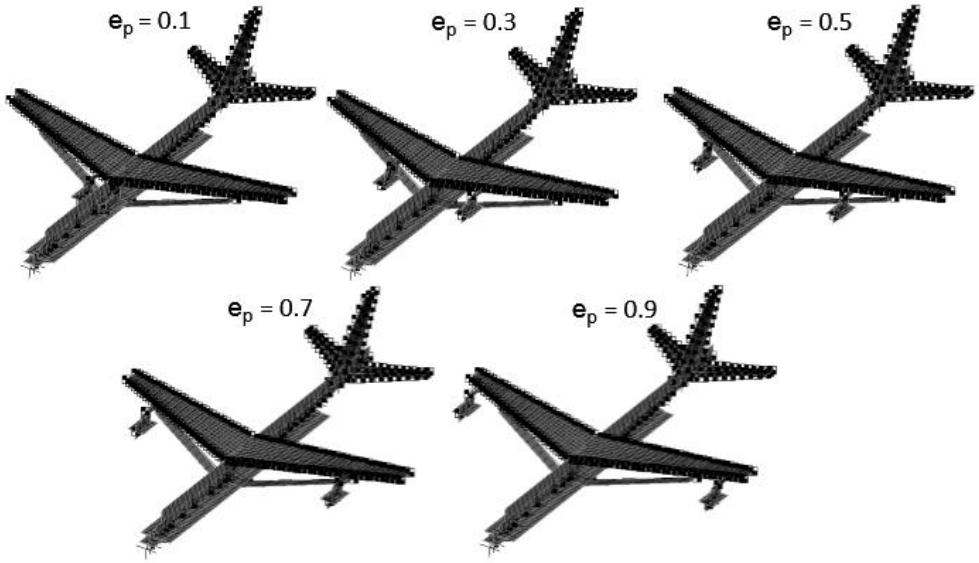

Figure 6: DLM and FEM model of the SBW with engine position variation.

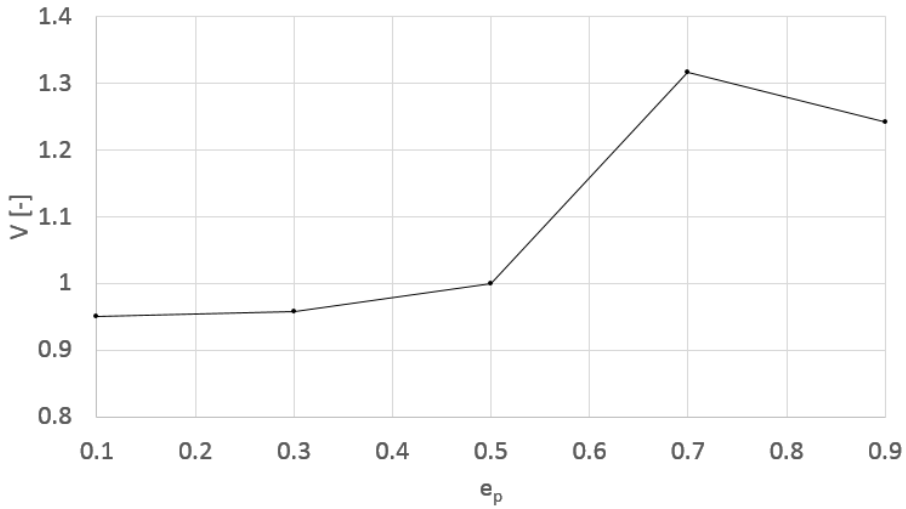

Figure 7: Nondimensional flutter speed as a function of spanwise engine position.

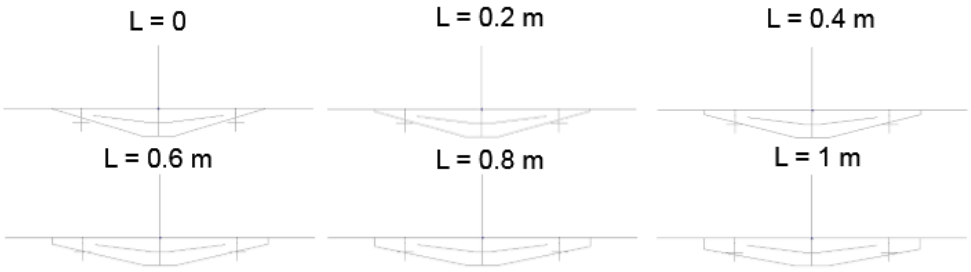

Figure 8: DLM model of the SBW with strut offset length variation.

The spanwise wing and strut intersection point was also analyzed, from values of 0.3 to 0.7. The geometric variations can be seen in Figure 12. As the length of the strut increases, since the area is kept constant, the strut chord decreases.

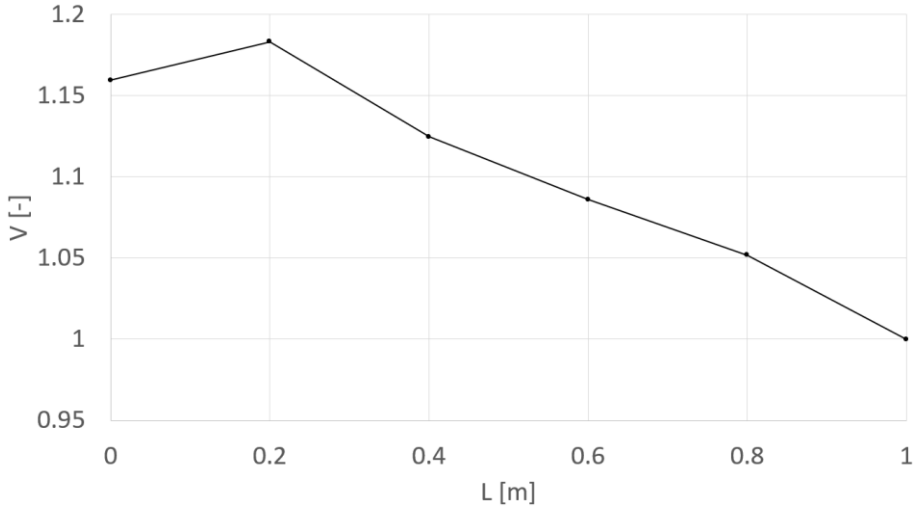

Figure 9: Nondimensional flutter speed as a function of strut offset length.

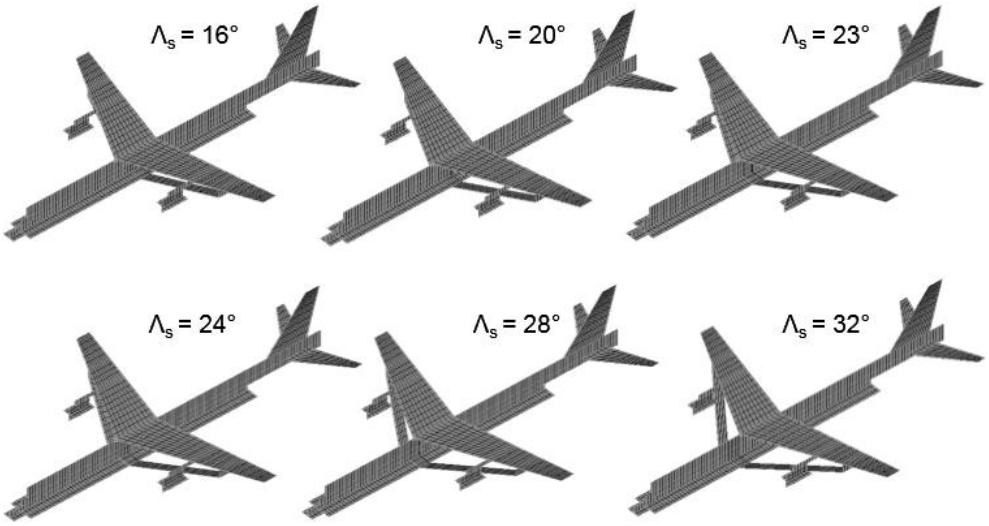

Figure 10: DLM model of the SBW with strut sweep angle variation.

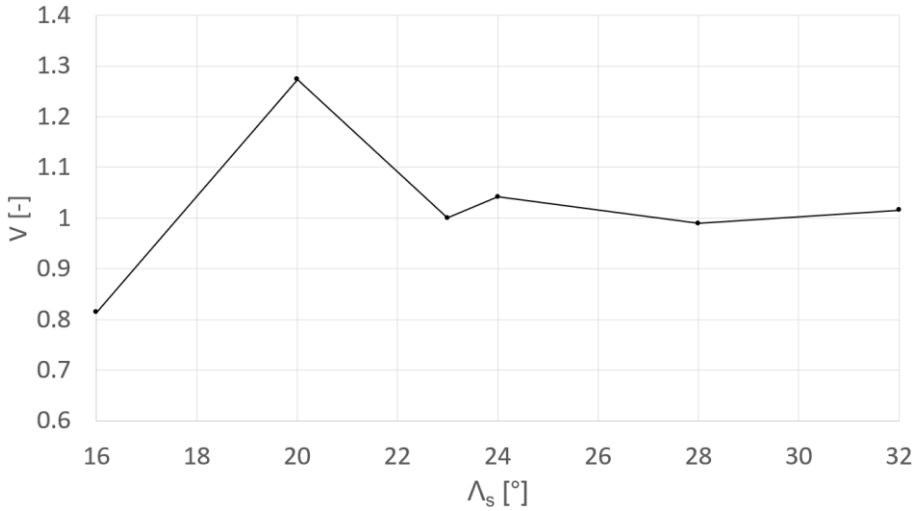

Figure 11: Nondimensional flutter speed as a function of strut sweep angle.

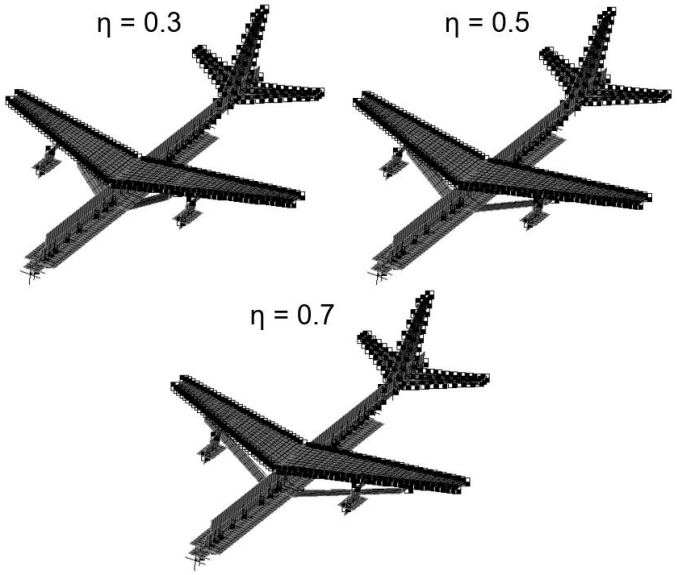

Figure 12: DLM and FEM model of the SBW with spanwise wing and strut intersection variation.

The results can be seen in Figure 13. A comparable behavior was obtained by Sulaeman [5], where the lowest flutter speed was also obtained for $\eta = 0.7$. Hence, for the range considered, the longer the strut, the lower the overall stiffness of the structure. This might be aggravated by the decreasing of the chord due to the increasing of the span.

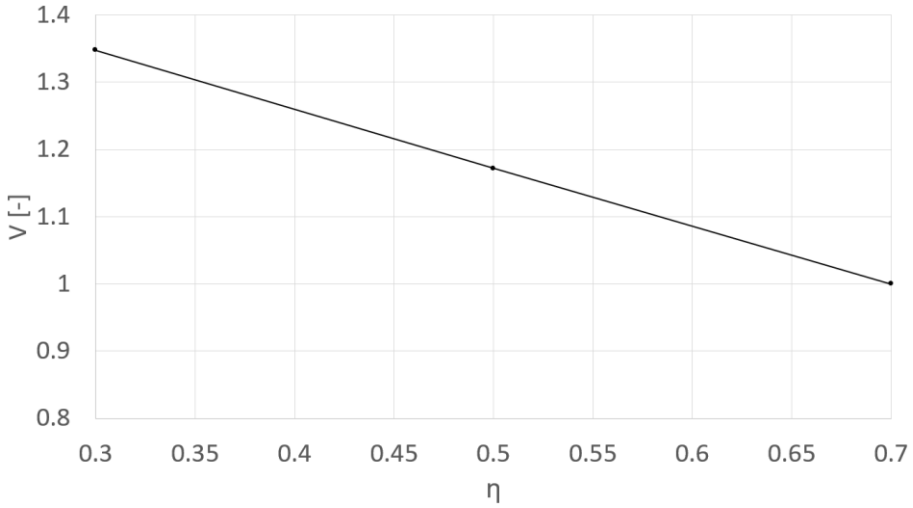

Figure 13: Nondimensional flutter speed as a function of spanwise wing and strut intersection.

The next parameter analyzed was the wing sweep angle, which was varied from 16° to 28°. These geometric variations can be seen in Figure 14. It is interesting to note that the strut sweep angle is maintained constant for these cases, however the point of intersection between strut and fuselage changes. The results can be seen in Figure 15, where it can be observed that as the wing sweep angle increases, the flutter speed increases. Even though the results seem to show a linear trend, the flutter mechanism observed for each case is different.

The next analysis consists of a variation of the wing taper ratio. The DLM and FEM models for each of the geometries analyzed can be seen in Figure 16. The results can be seen in Figure 17. The higher the taper ratio, the lower the flutter speed. One possible explanation for

this behavior is that as the taper ratio decreases, the aerodynamic loads on the wing tip are lower, requiring a higher speed to induce instabilities.

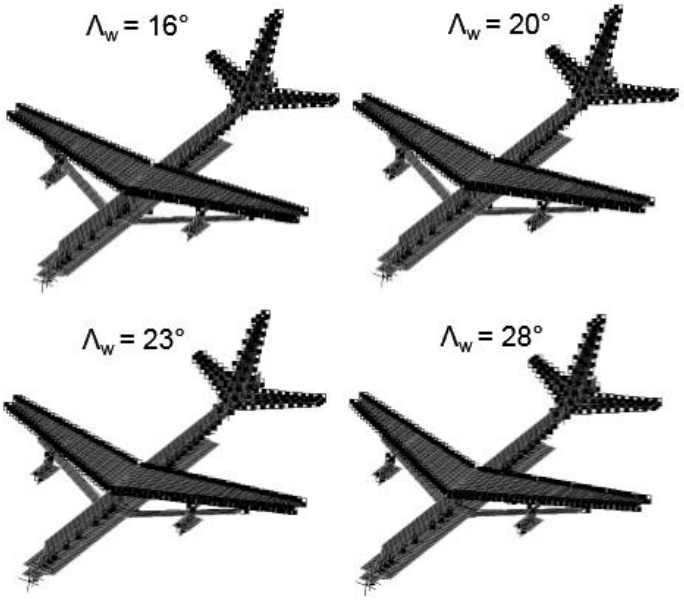

Figure 14: DLM and FEM model of the SBW with wing sweep angle variation.

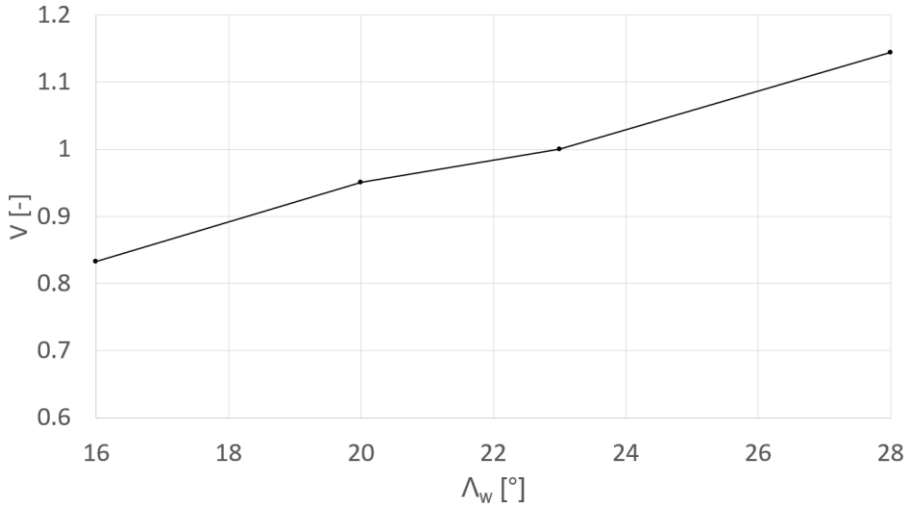

Figure 15: Nondimensional flutter speed as a function of wing sweep angle.

The influence of the strut force was also analyzed. The strut force is directly correlated the strut structural cross-sectional area. This analysis is performed with and without the consideration of the pre-stress that the strut is causing on the structure. It is important to note that in both analyses still only linear effects are being considered.

The results of the modal analysis showed that, even for the worst cases, there was not much difference between considering this preload for the flight condition analyzed. A Modal Assurance Criterion (MAC) analysis was performed for all geometric variations, and as can be seen for a strut force of 450000 N in Figure 18, there was little change in the mode shapes. Furthermore, mode frequencies changed less than 1%.

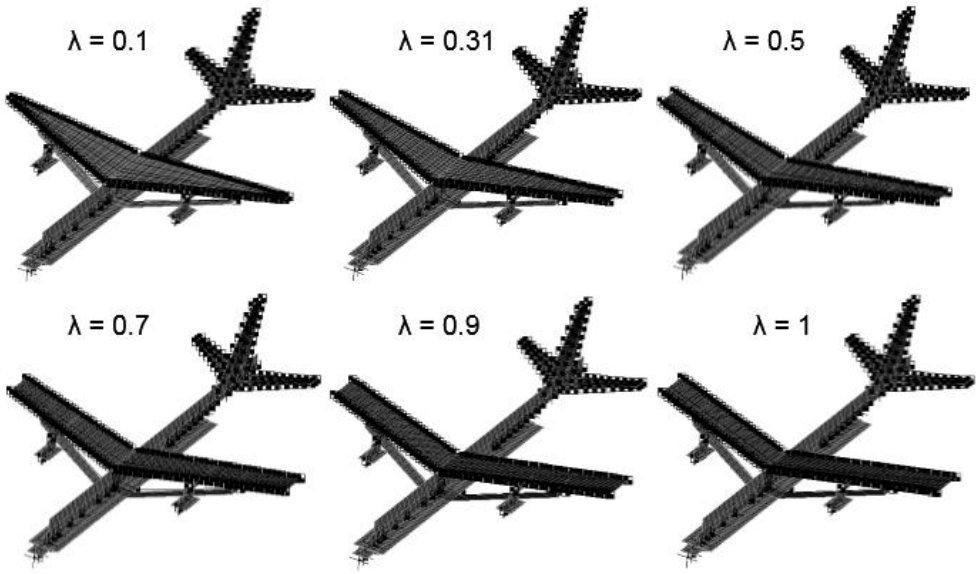

Figure 16: DLM and FEM model of the SBW with wing taper ratio variation.

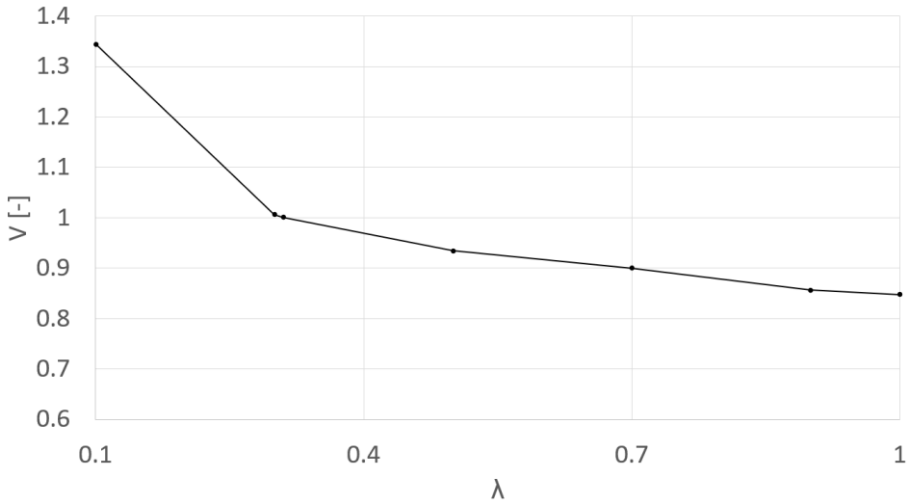

Figure 17: Nondimensional flutter speed as a function of wing taper ratio.

Little difference is expected in flutter speed results with the addition of the pre-stress. The results for the variation of the strut force can be seen in Figure 19. For this case, whenever there is a change in the trend of the curve, a change in the flutter mechanism is observed. However, small, almost irrelevant, variations are obtained. It is believed that if nonlinear and buckling effects are considered, a different behavior and higher variations might be observed, as concluded by Sulaeman [5], where it is stated that the wing buckling effect can be significant to the flutter speed, specially if the wing and strut intersection is located near the wing tip.

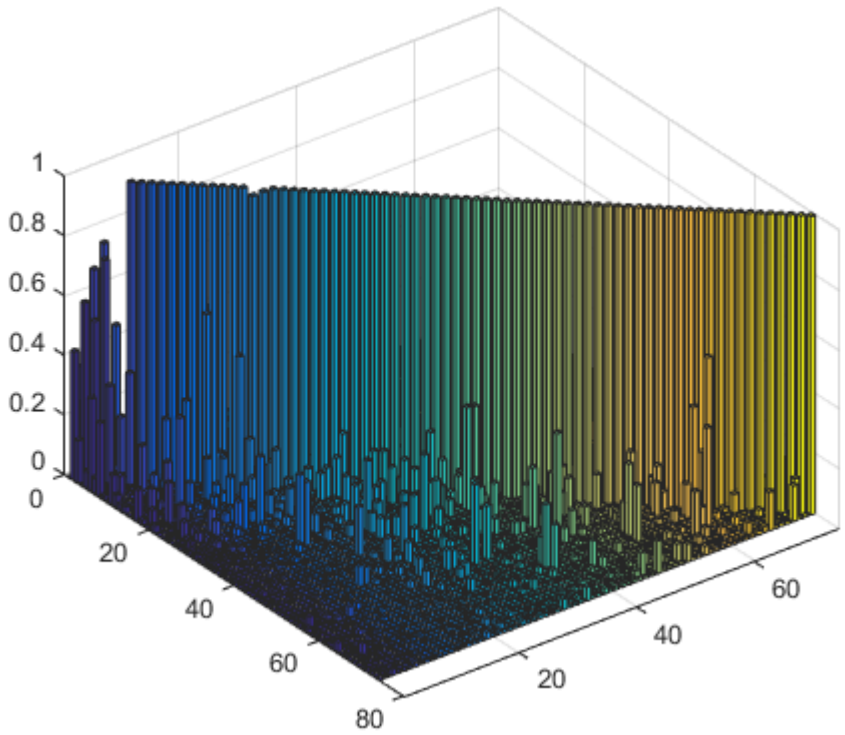

Figure 18: MAC analysis comparison between models with and without preload consideration.

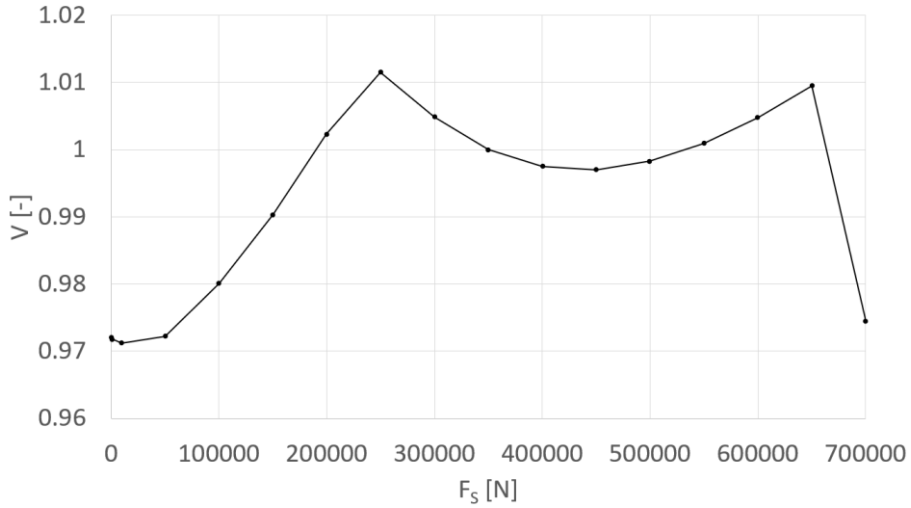

Figure 19: Nondimensional flutter speed as a function of strut force.

4 CONCLUSION

Regarding the aeroelastic behavior, for the strut braced wing aircraft configuration it is suggested that wings of lower aspect ratio, where the engine is positioned as close to the wing and strut intersection as possible, with a small strut offset, where the wing and strut intersection is close to the wing root, and with a high wing sweep angle and low taper ratio are considered. These observations should not be used as designing guidelines of the SBW configuration, but as points of attention.

Quantitavely, it was observed that: (a) increasing the wing aspect ratio from 8.3 to 12 decreases the flutter speed in 20%; (b) if the engine is positioned exactly at the wing and strut intersection at 70% of the wing span instead of 50%, an increase of 30% in flutter speed is obtained; and (c) the flutter speed can be increased by 35% if the spanwise wing and strut intersection is moved from 70% of the span to 30%.

The consideration of pre-stress on the structure should not be regarded as not necessary, even though the results obtained show no considerable changes. Other flight conditions could be analyzed, as well as higher forces and the location of these forces on the structure.
It is important to note that these results were obtained with variations of one parameter at a time hence, different trends could be observed in other cases.

5 ACKNOWLEDGMENTS

Thanks to Roberto da Mota Girardi, for advising early on this work. Thanks to Marcelo Nogueira for evaluating and advising on the aeroelastic model and Rodrigo França de Oliveira Marques for insights on the pre-stress consideration.

6 REFERENCES

[1] Meinicke, A. C., Rodrigues, J. C. M., da Silva, R. G. A. and Guedes, P. L. (2017). *Parametric Drag Analysis of Strut Braced Wing Aircraft for Regional Aviation*. In *Proceedings of the 24th ABCM International Congress of Mechanical Engineering – COBEM 2017*. Curitiba, Brazil.

[2] Bhatia, M., Kapania, R. K., van Hoek, M. and Haftka, R. T. (2009). *Structural Design of a Truss Braced Wing: Potential and Challenges*. In *Proceedings of the 50th Structures, Structural Dynamics, and Materials Conference*. Palm Springs, California.

[3] Bhatia, M., Kapania, R. K. and Haftka, R. T. (2012). *Structural and Aeroelastic Characteristics of Truss-Braced Wings: A Parametric Study*. Journal of Aircraft, v. 49, n. 1, p. 302-310.

[4] Coggin, J. M., Kapania, R. K., Zhao, W., Hodigere-Siddaramaiah, J. A. S., Allen, T. J. and Sexton, B. W. (2014). *Nonlinear Aeroelastic Analysis of a Truss Braced Wing Wind Tunnel Model*. AIAA SciTech, n. AIAA2014-0335. National Harbor, Maryland.

[5] Sulaeman, E. (2001). *Effect of Compressive Force on Aeroelastic Stability of a Strut-Braced Wing*. Ph.D. Thesis, Virginia Polytechnic Institute and State University, Blacksburg.

[6] Guimarães Neto, A. B. (2014). *Flight Dynamics of Flexible Aircraft Using General Body Axes: A Theoretical and Computational Analysis*. Ph.D. Thesis, Instituto Tecnológico de Aeronáutica, São José dos Campos, Brazil.

[7] Nagshineh-Pour, A. (1998). *Structural Optimization and Design of a Strut-Braced Wing Aircraft*. Master's Thesis, Virginia Polytechnic Institute and State University, Blacksburg.

[8] Rodden, W. P., Taylor, P. F., McIntosh, S. C. and Baler, M. L. (1999). *Further Convergence Studies of the Enhanced Doublet-Lattice Method*. Journal of Aircraft, v. 36, n. 4. P. 682-688.

[9] Tétrault, P. A. (2000). *Numerical Prediction of the Interference Drag of a Streamlined Strut Intersecting a Surface in Transonic Flow*. Ph.D. Theses, Virginia Polytechnic Institute and State University, Blacksburg.

[10] Duggirala, R. K., Roy, C. J. and Schetz, J. A. (2009). *Analysis of Interference Drag for Strut-Strut Interaction in Transonic Flow*. In *Proceedings of the AIAA Aerospace Sciences Meeting including The New Horizons Forum and Aerospapce Exposition.* Orlando, Florida.

[11] Seber, G., Ran, H., Schetz, J. A. and Mavris, D. N. (2011). *Multidisciplinary Design Optimization of a Truss Braced Wing Aircraft With Upgraded Aerodynamic Analyses.* In *Proceedings of the 29th AIAA Applied Aerodynamics Conference.* No. AIAA 2011-3179. Honolulu, Hawaii.

COPYRIGHT STATEMENT